Strong neuroprotection with a novel platinum nanoparticle against ischemic stroke- and tissue plasminogen activator-related brain damages in mice

Motonori Takamiya, MD; Yusei Miyamoto, PhD*; Toru Yamashita, MD, PhD; Kentaro Deguchi, MD, PhD; Yasuyuki Ohta, MD, PhD; Koji Abe, MD, PhD

From Department of Neurology, Okayama University Graduate School of Medicine, Dentistry and Pharmaceutical Sciences, 2-5-1 Shikatacho, Okayama 700-8558, Japan.

*From Department of Integrated Biosciences, Graduate School of Frontier Sciences, University of Tokyo, Bioscience Building 402, 5-1-5 Kashiwanoha, Kashiwa, Chiba 277-8562, Japan.

Corresponding author: Motonori Takamiya, M.D., Department of Neurology, Okayama University Graduate School of Medicine, Dentistry and Pharmaceutical Sciences, 2-5-1 Shikatacho, Okayama 700-8558, Japan.

Phone: +81-86-235-7365

Fax: +81-86-235-7368

E-mail: motonori@cc.okayama-u.ac.jp

Abbreviations used: blood-brain barrier (BBB), bovine serum albumin (BSA), caudate putamen (CPu), cerebral blood flow (CBF), hematoxyline-eosin (HE), hydroethidine (HEt), matrix metalloproteinase (MMP), middle cerebral artery (MCA), near-infrared fluorescence (NIRF), neurovascular unit (NVU), phosphate-bufferd saline (PBS), physiological saline (PS), platinum nanoparticle (nPt), reactive oxygen species (ROS), relative ratio (RR), standard deviation (SD), superoxide anions (SA), tissue plasminogen activator (tPA), transient middle cerebral artery occlusion (tMCAO), transillumination fluorescence imaging (TFI), 2,3,5-triphenyltetrazolium chloride (TTC)

Abstract

Reactive oxygen species (ROS) are major exacerbation factor in acute ischemic stroke, and thrombolytic agent tissue plasminogen activator (tPA) may worsen motor function and cerebral infarcts. The platinum nanoparticle (nPt) is a novel ROS scavenger, and thus we examined the clinical and neuroprotective effects of nPt in ischemic mouse brains. Mice were subjected to transient middle cerebral artery occlusion (tMCAO) for 60 min and divided into the following four groups by intravenous administration upon reperfusion, vehicle, tPA, tPA+nPt, and nPt. At 48 hrs after tMCAO, motor function, infarct volume, immunohistochemical analyses of neurovascular unit (NVU), in vivo imaging of matrix metalloproteinase (MMP), and zymography for MMP-9 activity were examined. Superoxide anion generation at 2 hrs after tMCAO was also examined with hydroethidine. As a result, administration of tPA deteriorated the motor function and infarct volume as compared to vehicle. In vivo optical imaging of MMP showed strong fluorescent signals in affected regions of tMCAO groups. Immunohistochemical analyses revealed that tMCAO resulted in a minimal decrease of NAGO and occludin, but a great decrease of collagen IV and a remarkable increase of MMP-9. Hydroethidine stain showed increased ROS generation by tMCAO. All these results became pronounced with tPA administration, and were greatly reduced by nPt. The present study demonstrates that nPt treatment ameliorates neurological function and brain damage in acute cerebral infarction with neuroprotective effect on NVU and inactivation of MMP-9. The strong reduction of ROS

production by nPt could account for these remarkable neurological and neuroprotective effects against ischemic stroke.

Key Words: platinum nanoparticle, cerebral ischemia, free radical scavenger, neuroprotection, matrix metalloproteinase-9, tissue plasminogen activator

1. Introduction

Acute ischemic stroke is a major cause of death and, even when not fatal, usually results in permanent neurological impairments, for which both blood flow improvement and neuroprotective therapies are critical. A thrombolytic agent, tissue plasminogen activator (tPA), has been used for the treatment of acute cerebral infarction, but its application is limited due to the narrow therapeutic time window and side effect of hemorrhagic transformation (Tsirka et al., 1995; Wang et al., 1998; Nagai et al., 1999; Kilic et al., 2005; Ning et al., 2006; Yamashita et al., 2009; Abu et al., 2010). Intravenous tPA treatment has been limited to within 3 hrs after the onset of ischemic stroke, but recent clinical evidence provided an extension of the time window from 3 to 4.5 hrs (Wahlgren et al., 2008; Lansberg et al., 2009). However, the extension also increased the risk of hemorrhagic complications (Wahlgren et al., 2008; Lansberg et al., 2009), which further increases the demand for neuroprotection to reduce the risk of harmful cerebral hemorrhage.

The generation of reactive oxygen species (ROS) starts soon after vessel occlusion and propagates explosively after reperfusion (Chan, 2001). These ROS have been proved to be of key importance in the pathogenesis of ischemic brain injury (Kinouchi et al., 1991; Kontos, 2001). We originally reported that a free radical scavenger edaravone strongly ameliorated edema in the ischemic brain (Abe et al., 1988) and reduced the infarct size and free radical end products of lipids, proteins, and DNA (Zhang et al., 2004). Because edaravone strongly improved the

disability after ischemic stroke without serious adverse events (The Edaravone Acute Brain Infarction Study group, 2003), it has been used in clinical therapy for ischemic stroke in Japan from 2001. We have furthermore reported the strong neuroprotective effect of edaravone especially in preserving neurovascular units (NVU) after cerebral ischemia in the stroke-prone spontaneously hypertensive rat (Yamashita et al., 2009). Besides edaravone, we have also reported that ischemic brain damage was ameliorated by other neuroprotective substrates such as HMG-CoA reductase inhibitor statins (Hayashi et al., 2005; Nagotani et al., 2005), antihypertensive azelnidipine (Lukic-Panin et al., 2007), and biliverdin (Deguchi et al., 2008) after ischemic stroke.

Platinum nanoparticle (nPt) species have been reported as novel free radical scavengers which strongly ameliorate oxidative damage in vitro and in vivo (Kim et al., 2008, 2010; Onizawa et al., 2009; Watanabe et al., 2009; Sakaue et al., 2010; Takamiya et al., 2011). Due to the larger surface area-to-volume ratio of smaller particles, nPt can potentiate the catalytic activity of metals, and its colloidal forms contribute to a further efficient catalysis with high electron holding at the surface (Roucoux et al., 2002), allowing it to quench both superoxide anion and hydrogen peroxide (Kajita et al., 2007; Hamasaki et al., 2008). We have previously reported that administration of nPt could be beneficial for clinical improvement and neuroprotection in the pathological aspects of mice after transient middle cerebral artery occlusion (tMCAO) (Takamiya et al., 2011), and in the present study, we further investigated the efficacy of nPt associated with tPA administration.

2. Experimental procedures

2.1.1. Animal model

Male C57/Bl6 mice (Japan SLC Inc, Shizuoka, Japan, 8 weeks old, weighing 24-27 g) were anesthetized with an nitrousoxide/oxygen/isofluran mixture (69: 30: 1%) during surgical preparation. tMCAO was induced by the intraluminal filament technique according to our previous report (Lukic-Panin et al., 2007; Abe et al., 1992; Yamashita et al., 2006). In brief, the right common carotid artery was isolated and a small incision was made for thread insertion. Then, 8-0 nylon thread with a silicon-coated tip was inserted into the right MCA and gently advanced 9.0-10.0 mm to occlude the origin of MCA. During these surgical treatments and subsequent ischemic period, body temperature was monitored to maintain a temperature of 37 ± 0.3°C by placing animals on a heating bed (Model BWT-100; Bio Research Center, Nagoya, Japan). Regional CBF in the ischemic area was estimated by measuring blood flow at partial resection of the scalp 1 mm posterior and 3 mm lateral to the bregma with a laser-Doppler flow meter (FLO-C1; Omegawave, Tokyo, Japan). CBF was monitored at a baseline time point before the ischemic operation, at 5 and 10 min after the cerebral ischemia, and at 5 min after the reperfusion, as described in our previous reports (Lukic-Panin et al., 2007; Yamashita et al., 2006). At 60 min after tMCAO, the nylon thread was withdrawn for reperfusion, followed by intravenous administration of the drug as described below in detail. After the incision was closed, the animals recovered and were allowed free access to water and food at an ambient temperature (21-23°C) until motor function evaluation, in vivo imaging, and subsequent brain sampling for

ex vivo imaging, infarction volume determination, zymography, and immunohistochemistry. The experimental protocol and procedure were approved by the Animal Committee of the Graduate School of Medicine and Dentistry, Okayama University.

2.1.2. Preparation and administration of drug and 5 mice groups

The nPts were prepared by ethanol reduction of $H_2PtCl_6 \cdot 6H2O$ as described previously (Kim et al., 2008). Poly (*N*-vinyl-2-pyrrolidone) was used as a protecting reagent to prepare an evenly dispersed suspension. The nPts were dissolved in physiological saline (PS) and stored at 4°C until use.

The mice were divided into 5 groups, the sham control group receiving only a surgical sham operation without thread insertion (total n=12: 3 for motor function assessment with subsequent infarction volume determination and immunohistochemistry, 3 for in vivo and ex vivo optical imaging of MMP, 3 for zymography, and 3 for detection of superoxide anion), the tMCAO-vehicle group receiving only a vehicle (PS administered from tail vein at 10 mL/kg of mouse) at the time of reperfusion after 60 min of tMCAO (total n=21: 12, 3, 3, and 3), the tMCAO-tPA (Alteplase, Mitsubishi Tanabe Pharma Corporation, Osaka, Japan, intravenously, 10mg/kg) group receiving tPA at reperfusion (total n=17: 8, 3, 3, and 3), tMCAO-tPA+nPt group receiving nPts (4.0 μmol/kg of mouse) just after tPA administration at reperfusion (total n=17: 8, 3, 3, and 3), and tMCAO-nPt group receiving nPts at reperfusion (total n=19: 10, 3, 3, and 3). The administration volume of each group was approximately 0.3 ml according to the weight of

the mice.

2.2.1. Behavioral analysis

At 48 hrs after the reperfusion, the mice were evaluated by behavioral tests as described by Bederson (Bederson et al., 1986) with our minor modifications (Yamashita et al., 2009) as follows: 0, no observable neurologic deficits; 1, failure to extend the right forepaw; 2, circling to the contralateral side; 3, falling to the right; 4, unable to walk spontaneously. After Bederson's test, a rota-rod test (MK-610A, MUROMACHI KIKAI CO., LTD) was performed 3 times with an accelerating spindle speed from 5 to 45 rpm over a period of 1 min. The scoring was carried out blind to each condition.

2.2.2. Measurement of infarct volume

After finishing behavioral analysis, the mice were anesthetized again by intraperitoneal injection of pentobarbital (40 mg/kg), and transcardially perfused with chilled 5 U/ml heparin in phosphate-bufferd saline (PBS), followed by 4% paraformaldehyde in 0.1 M sodium phosphate buffer (pH 7.4). Subsequently, brains were removed, immersed with 4% paraformaldehyde in PBS over night at 4,°C and subjected to consecutive incubation with 10, 20 and 30% sucrose in PBS. Each sucrose incubation step was for 24 hrs at 4°C. Then, the treated brains were rapidly frozen in dry ice for preparation of 20 μm thick coronal sections at the caudate level with a cryostat maintained at -20°C. The sliced sections were mounted on silane-coated slide glasses.

Coronal brain sections of these mice were stained with HE to quantify infarct volume with a standard computer-assisted image analysis technique. The total infarct volume of the cerebral cortex or CPu for each brain was calculated by summation of the infarcted area of 7 serial brain slices, at a 500 μm interval each, between 1.0 mm anterior, and 2.0 mm posterior, to the bregma. To eliminate the contribution of postischemic edema, infarct volume measurements were corrected as previously described (Kitano et al., 2004).

2.3.1. In vivo optical imaging of matrix metalloproteinase

Mice were subjected to in vivo imaging at 48 hrs after the tMCAO. The fluorescent compound MMPSense 680 (VisEn Medical Inc., USA) was used in this experiment for testing matrix metalloproteinases (MMPs including MMP-2, -3, the key -9 and -13). MMPSense (300 μl) was intravenously injected 12 hrs before the in vivo imaging (i.e., 36 h after tMCAO). For in vivo imaging, the mice were anesthetized with a nitrous oxide/oxygen/isoflurane mixture (69/30/1%) administered through an inhalation mask, and the near-infrared fluorescence (NIRF) images were observed by a macro fluorescence imaging system as described above with or without the head skin.

For in vivo imaging, we used the macro fluorescence imaging system MVX 10 Macro View (Olympus, Japan). For excitation of fluorescent compounds, an intensity-controlled laser diode emitting at 682 nm was used. The fluorescence emission at 721 nm was collected by a

charge-coupled device (CCD) camera (Digital camera C10600 ORCA-R2, Hamamatsu, Japan) with an acquisition time of 3.0 sec. The transillumination fluorescence images (TFI) were analyzed by MetaMorph Version 7.5 image analysis software.

2.3.2. Ex vivo optical imaging of matrix metalloproteinase

After taking in vivo images, the mouse brains were removed under deep anesthesia with pentobarbital (40 mg/kg, i.p.), and ex vivo imaging for MMP was quickly performed as above. Just after ex vivo imaging of the tMCAO-tPA-treated mouse brains, immunofluorescent staining of MMP-9 was performed with the primary antibody for MMP-9 (1:200; R&D SYSTEMS, Minnesota) and secondary antibody conjugated with Alexa Fluor 488 (1:500; Invitrogen, CA) to confirm that the fluorescence actually represents MMP. Using another set of tMCAO-tPA treated mice (n=3), TTC stain was also performed after obtaining ex vivo images with MMPSense.

2.4. Immunohistochemistry

As described above, coronal brain sections of 20 μm thickness at the caudate level were cut and mounted on silane-coated slide glasses. The sections were first washed in PBS and then incubated with 30% methanol and 0.3% hydrogen peroxide in PBS in order to quench endogenous peroxide activity. After non-specific reactions were blocked by 5% bovine serum

albumin (BSA) in PBS for 1 hr, the slides were incubated overnight at 4°C with the primary antibody in 5% BSA in PBS. Then, the slides were washed in PBS and incubated for 1 hr with an appropriate biotin-labeled secondary antibody (1:500) at room temperature. They were subsequently incubated with an avidin-biotin-peroxide complex (Vector Laboratories, Burlingame, CA) for 30 min and the signal was visualized with diaminobenzidine tetrahydrochloride. The primary antibodies in this study were as follows: anti-MMP-9 (1:200; R&D SYSTEMS, Minnesota), anti-collagen IV (1:100; NOVOTEC, Lyon, France), anti-occludin (1:100; SANTA CRUZ Biotechnology, CA), and NAGO (1:200; Vector Laboratories, Burlingame, CA). In each study, sections were stained in a similar way without the primary antibody as a negative control.

2.5. Gelatine zymography

At 48 hrs after reperfusion, mice were anesthetized by intraperitoneal injection of pentobarbital (40 mg/kg) and transcardially perfused with chilled 5 U/ml heparin in PBS. Brains were removed quickly and divided into ipsilateral-ischemic and contralateral-nonischemic hemispheres. Each hemispheric brain was frozen immediately in dry ice and stored at -80°C until use.

Brain samples were homogenized in a 10 × volume lysis buffer (150 mM NaCl, 1% SDS, 0.1% deoxycholic acid, and 50 mM Tris-HCl, pH 7.4) containing protease inhibitors. After centrifugation at 9,000 × g for 15 min at 4°C, the supernatant was collected. The total protein

concentration of each supernatant sample was spectrophotometrically determined using the Bradford assay (Ultrospec 3100 pro, GE Healthcare, Tokyo, Japan). The MMP-9 activity of each sample was measured using a gelatin-zymography kit (Primary cell, Sapporo, Japan) according to the manufacturer's instructions. In brief, each sample containing 20 μg protein was diluted with the homogenizing buffer in the kit, mixed with an equal volume of sample buffer, and loaded for the electrophoresis for 2 hrs. The gels were washed and incubated for 24 hrs with the incubation buffer at 37°C. The gels were stained with Coomassie blue and scanned. Quantitative densitometric analysis was performed using ImageJ software.

2.6. Detection of superoxide anions (SA) and double immunofluorescent analysis

Production of SA in the mouse brains after 60 min of tMCAO was investigated by in situ detection with oxidized hydroethidine (HEt) as described previously (Sugawara et al., 2002). Intravenously-administered HEt (Molecular Probes, Eugene, OR) is taken up by living cells and oxidized by SA to produce a red fluorescent dye, ethidium (Bindokas et al., 1996). In the present experiment, 0.1 ml of 1 mg/ml HEt in PS containing 1% dimethylsulfoxide was administered via the tail vein at 60 min after tMCAO. At 60 min after the drug administration, mice were anesthetized by intraperitoneal injection of pentobarbital (40 mg/kg) and transcardially perfused with chilled 5 U/ml heparin in PBS, followed by 4% paraformaldehyde in 0.1 M phosphate buffer (pH 7.4). The brains were then removed, immersed with 4% paraformaldehyde in PBS overnight at 4°C, and rapidly frozen in dry ice. Twenty micrometer thick coronal sections were

cut at the caudate level with a cryostat kept at -20°C and mounted on silane-coated slide glasses.

Immunofluorescent analysis was performed to investigate the ROS-production level of each cell component constituting brain tissue. The sections were first washed in PBS and after non-specific reactions were blocked by 5% BSA in PBS for 1 hr, the slides were incubated overnight at 4°C with the primary antibody in 5% BSA in PBS. The slides were then washed in PBS and incubated for 1 hr with an appropriate secondary antibody at room temperature. The primary antibodies in this study were as follows: anti-CD31 (1:50; BD Biosciences, CA) for endothelium, anti-MAP2 (1:200; MILLIPORE, CA) for neuron, anti-GFAP (1:200; Glostrup, Denmark) for astrocyte, and anti-IBA1 (1:200; Wako Pure Chemical Industries, Osaka, Japan) for microglia. In each study, sections were stained in a similar way without the primary antibody as a negative control. The secondary antibodies were as follows: Alexa Fluor 350 (1:500; Invitrogen, CA) for anti-CD31 antibody, and Alexa Fluor 488 (1:500;Invitrogen, CA) for anti-MAP2, -GFAP, -IBA1 antibodies, respectively. The slides were covered with VECTASHIELD mounting medium (Vector Laboratories, Burlingame, CA) and the peri-infarction areas were observed with a fluorescence stereomicroscope (Olympus FLUOVIEW FV10i; Olympus Optical Co., Tokyo, Japan). The mean signal intensity randomly chosen in 10 fields of peri-infarction area were quantified using computer software MetaMorph® (Molecular Devices Corporation, Sunnyvale, CA). The data of mean signal intensity are presented as Unit/area. We have quantified the Ethidium fluorescence ratiometrically as follows. First semiquantitative fluorescence were measured in the anatomically comparable sites of

contralateral hemisphere with the peri-infarct region of ipsilateral hemisphere by calculating the sum of integral intensity using the image analysis software, then we confirmed that there were no significant difference in the fluorescent signal intensity between sham control and each tMCAO groups. Subsequently integral fluorescent signal intensity of contralateral site comparable to peri-infarct region of ipsilateral hemisphere were hence subtracted to correct for background.

2.7. Statistical analysis

Results are presented as the mean ± standard deviation (SD). Statistical comparisons were conducted using Mann-Whitney tests followed by Kruskal-Wallis tests for intergroup comparisons. A probability value of $p < 0.05$ was considered statistically significant.

3. Results

3.1. Cerebral blood flow (CBF)

After tMCAO, CBF immediately dropped to less than 30% of the baseline. With reperfusion, CBF quickly recovered to the basal level in all groups (i.e. tMCAO-vehicle, tMCAO-tPA, tMCAO-tPA+nPt and tMCAO-nPt groups). Throughout these tMCAO experiments, there was no significant difference in CBF between all groups (data not shown).

3.2. Motor function and infarct volume

To evaluate motor function in the mice at 48 hrs after 60 min of tMCAO, Bederson's and rota-rod tests were performed. Bederson's grades of the sham control, tMCAO-vehicle, tMCAO-tPA, tMCAO-tPA+nPt, and tMCAO-nPt groups were 0 ± 0 (mean ± standard deviation), 2.17 ± 0.39**, 2.38 ± 0.52**, 1.63 ± 0.52$^{\star\star,*,\#}$ and 1.10 ± 0.57**,**, respectively ($\star\star p < 0.01$ vs sham control group, $*p < 0.05$, $**p < 0.01$ vs tMCAO-vehicle group, $\#p < 0.05$ vs tMCAO-tPA group; Fig. 1A). Rota-rod scores of the above 5 groups were 44.3 ± 15.3 (sec), 17.3 ± 5.4**, 11.9 ± 3.8**,*, 21.7 ± 8.5$^{\star\star,\#}$, and 29.9 ± 9.0 ,**, respectively ($\star\star p < 0.01$ vs sham control group, $*p < 0.05$, $**p < 0.01$ vs tMCAO-vehicle group, $\#p < 0.05$ vs tMCAO-tPA group; Fig. 1B).

Hematoxyline-eosin (HE) -stained sections at 48 hrs after 60 min of tMCAO showed that the infarct volumes at the cerebral cortex in the tMCAO-vehicle and -nPt groups were 30.1 ± 5.2 (mm^3), 38.2 ± 5.7**, 22.1 ± 6.3$^{*,\#\#}$, and 17.3 ± 6.8** ($*p < 0.05$, $**p < 0.01$ vs tMCAO-vehicle group, $\#\#p < 0.01$ vs MCAO-tPA group), and at the caudoputamen (CPu) were 9.2 ± 1.3, 9.2 ±

0.9, 7.5 ± 1.5*,# and 7.3 ± 1.2** (p = n.s.), respectively (*p < 0.05, **p < 0.01 vs tMCAO-vehicle group, #p < 0.05 vs MCAO-tPA group) (Fig. 1C).

3.3. In vivo and ex vivo optical imaging of matrix metalloproteinase

The in vivo fluorescent optical signal of matrix metalloproteinase (MMP) was scarcely detected with scalp and hair, but became clearly detected through skull bone by removing the scalp. Fig. 2A demonstrates the in vivo optical image of MMP at 48 hrs after tMCAO by near-infrared fluorescence (NIRF) observation of fluorescent compounds using MMPSense 680 (upper panels for non-fluorescence observation, and the lower panels for pseudocolor image). There was almost no fluorescence over the sham control head, but clear fluorescence was observed in the affected hemisphere reflecting the right middle cerebral artery (MCA) territory, with signal strength in the order tMCAO-tPA > tMCAO-vehicle > tMCAO-tPA+nPt > tMCAO-nPt group (Fig. 2A; lower panels).

Fig. 2B and 2C demonstrate the ex vivo imaging of MMP just after the in vivo imaging of the whole brain (Fig. 2B, upper panels for non-fluorescence observation and lower for pseudocolor image of MMPSense 680) and brain slice (Fig. 2C, similar to Fig. 2B). Compared with in vivo imaging (Fig. 2A), the fluorescent signal became more evident in the affected right MCA territory, with signal strength again in the order tMCAO-tPA > tMCAO-vehicle > tMCAO-tPA+nPt > tMCAO-nPt group (Fig. 2B and 2C; lower panels).

Macroscopic comparison of brain sections with TTC stain and ex vivo MMP images in

identical tMCAO-tPA mice showed close colocalization of 2,3,5-triphenyltetrazolium chloride (TTC) stain defect (white area, Fig. 2D) and MMP image increase (yellow area, Fig. 2D). Microscopic examination confirmed the colocalization of endogenous MMPSense signal and exogenous MMP-9 antibody in the affected area (Fig. 2E).

3.4. Zymography for MMP-9 activity

There was only a trace level of MMP-9 activity in the sham control and contralateral brains of the tMCAO groups, which showed an evident increase in the ipsilateral hemisphere after tMCAO (Fig. 3A). As the reference of this sham control activity 1.00, relative ratio (RR) of the optical densities for MMP-9 in tMCAO-vehicle, tMCAO-tPA, tMCAO-tPA+nPt, and tMCAO-nPt in the contralateral hemisphere as 1.16 ± 0.40, 1.82 ± 1.01, 0.99 ± 1.00, and 1.20 ± 0.40, respectively, and those in the ipsilateral hemisphere as $5.30 \pm 0.88^{\star}$, $7.84 \pm 2.19^{\star,*}$, $3.04 \pm 1.77^{\star,\#}$ and $2.87 \pm 0.45^{\star,*}$, respectively ($^{\star}p < 0.05$ vs sham control group, $^{*}p < 0.05$ vs tMCAO-vehicle group, $\#p < 0.05$ vs tMCAO-tPA group) (Fig. 3B).

3.5. Immunohistochemistry for NVU

Staining for NAGO exhibited short linear structures with a few branches in the peri-infarct area of cerebral cortex, representing the vascular endothelium (Fig. 4, top panels). The relative ratio (RR) of mean signal intensities for NAGO staining of the sham control group (as RR = 1), tMCAO-vehicle, tMCAO-tPA, tMCAO-tPA+nPt and tMCAO-nPt group were 1.00 ± 0.09, 0.72

± 0.14**, 0.69 ± 0.07**, 0.79 ± 0.26, and 0.81 ± 0.16*, respectively ($\star p < 0.05$, $\star\star p < 0.01$ vs sham control group).

Staining for occludin also showed small linear structures with a few branches, representing the tight junction of neurovascular components (Fig. 4, second panels). The RR of signal intensities for occludin staining in these 5 groups were 1.00 ± 0.06, 0.72 ± 0.32**, 0.70 ± 0.19**, 0.81 ± 0.29, and 0.86 ± 0.31, respectively ($\star\star p < 0.01$ vs sham control group). The signal intensity tended to be lower in the tMCAO-vehicle and tMCAO-tPA group, but again no significant difference was found.

Staining for collagen IV also showed linear structures with a few branches, clearly representing the basal lamina of neurovascular components (Fig. 4, third panels). The RR of signal intensities of collagen IV of the sham control, tMCAO-vehicle, tMCAO-tPA, tMCAO-tPA+nPt, and tMCAO-nPt groups were 1.00 ± 0.08, 0.58 ± 0.32**, 0.30 ± 0.27**, 0.74 ± 0.23$^{\star,\#\#}$, and 0.85 ± 0.14*,* ($\star p < 0.05$, $\star\star p < 0.01$ vs sham control group, $*p < 0.05$ vs tMCAO-vehicle group, $\#\#p < 0.05$ vs tMCAO-tPA group), respectively. Collagen IV was significantly degraded at 48 hrs after 60 min of tMCAO, which tended to be exacerbated by tPA administration, and these degradation were significantly salvaged by the nPt-treatment.

Staining for MMP-9 showed several shapes such as a similar linear structure to NAGO, occludin and collagen IV, and its surrounding small dots (Fig. 4, bottom panels), representing the extracellular matrix and possibly cells generating MMP-9 in the peri-infarct area. The RR of signal intensities for the MMP-9 of the sham control, tMCAO-vehicle, tMCAO-tPA,

tMCAO-tPA+nPt, and tMCAO-nPt groups were 1.00 ± 0.24, 5.28 ± 1.25**, 9.97 ± 2.37**,**, 4.03 ± 1.23$^{\star\star,*,\#\#}$, and 2.32 ± 0.34**,** ($\star\star p < 0.01$ vs sham control group, $*p < 0.05$, $**p < 0.01$ vs tMCAO-vehicle group, $\#\#p < 0.01$ vs tMCAO-tPA group), respectively. MMP-9 staining was markedly increased at 48 hrs after tMCAO, which was exacerbated by tPA administration, and these marked increase were significantly inhibited by the nPt-treatment.

In all immunostainings above, no significant staining was found without a primary antibody, supporting the specific staining for each marker protein.

3.6. Evaluation of superoxide production

Although no signal was detected in the sham control brain, the tMCAO-vehicle and tMCAO-tPA groups showed strong signals at the peri-infarct area in the ipsilateral cerebral cortex of the MCA territory. This signal was markedly reduced in the tMCAO-tPA+nPt and tMCAO-nPt groups (Fig. 5A). Statistical analysis of these signals showed that the RR of the signal intensities for superoxide of the sham control, tMCAO-vehicle, tMCAO-tPA, tMCAO-tPA+nPt, and tMCAO-nPt groups were 1.0 ± 0.4, 14.0 ± 6.6**, 37.5 ± 12.2**,**, 6.5 ± 1.5$^{\star,\#}$, and 2.6 ± 0.2*,*, respectively ($\star p < 0.05$, $\star\star p < 0.01$ vs sham control group, $*p < 0.05$, $**p < 0.01$ vs tMCAO-vehicle group, $\#p < 0.05$ vs tMCAO-tPA group; Fig. 5A). Triple immunofluorescent analysis showed hydroethidine signals indicating the existence of superoxide predominantly in the endothelium (Fig. 5B, filled arrows) and at the peri-infarct area in the ipsilateral cerebral cortex of the MCA territory of tMCAO-vehicle and tMCAO-tPA groups with

less intensity with nPt treatments (Fig. 5B, open arrows). Small numbers of hydroethidine signals were also present in the outer margin of MAP2 fluorescence, suggesting a slight ROS production in the cytoplasmic membrane of peri-infarct neurons. The ROS production ratios of each cell component were as follows; the ratios of endothelium, neuron, microglia, and astrocyte were 95.1%, 2.0%, 2.9% and 0%, respectively in sham control group, 44.6%, 39.4%, 12.7%, and 3.2% in tMCAO-vehicle group, 53.1%, 36.5%, 6.1%, and 4.1% in tMCAO-tPA group, 79.2%, 14.1%, 1.7%, and 5.0% in tMCAO-tPA+nPt group, 94.1%, 2.0%, 2.8%, and 1.1% in tMCAO-nPt group, respectively (Fig. 5A).

4. Discussion

The generation of ROS gradually increases during cerebral ischemia, but explosively increases after reperfusion especially in the ischemic penumbra oxidising the lipid, DNA and proteins (Chan, 1996; Morimoto et al., 1996; Peters et al., 1998; Abe, 2000; Cui et al., 2000; Zhang et al., 2001). Thus the detrimental effects of ROS in cerebral ischemia-reperfusion injury are profoundly associated with the pathophysiology of neural cell apoptosis and necrotic infarction (Demopoulos, 1973; Hayashi et al., 1999). We have previously demonstrated the strong neuroprotective effects of a free radical scavenger edaravone (Yamashita et al., 2009; Abe et al., 1988; Yoneda et al., 2003), which has been clinically used as the world's first neuroprotective drug in Japan since 2001. Recent evidence suggested that other free radical scavengers such as biliverdin (Deguchi et al., 2008), 6-hydroxy-2,5,7,8-tetramethylchroman-2-carboxylic acid (trolox) (Perfeito et al., 2007; Sharma and Kaundal, 2007) and 2,2,5,7,8-pentamethyl-6-hydroxychromane (PMC) (Hsiao et al., 2007) also ameliorated cerebral injury following experimental tMCAO.

In the present study, we took a novel free radical scavenger nPts because of its double-scavenging property for superoxide anion and hydrogen peroxide. The size of nPt, ranging from 2-3 nm, is the most potent subclass of antioxidant for application in living bodies. Unlike common antioxidants such as ascorbic acid which lose their reduction effect when oxidized, the antioxidative effect of nPt is durable for its feature as both SOD/catalase mimetic (Kajita et al., 2007; Hamasaki et al., 2008). In in vivo application, nPt extended the lifespan of

the roundworm *Caenorhabditis ekegans* (Kim et al., 2008, 2010; Sakaue et al., 2010), inhibited pulmonary inflammation in mice exposed to cigarette smoke (Onizawa et al., 2009), and inhibited cell growth of human tongue carcinoma cells (Saitoh et al., 2009). Furthermore we have previously reported that nPt ameliorates neurological function and brain damage after tMCAO in mice (Takamiya et al., 2011). The present study confirmed these findings and additionally showed that nPt ameliorated the exacerbated damage caused by tPA in conjunction with tMCAO in mice.

Large quantities of ROS are generated in the peri-vascular extracellular space after cerebral ischemia (Kontos et al., 1992). Such ROS are important for MMP-9 activation which participates in early blood-brain barrier (BBB) disruption triggered by oxidative stress generated during cerebral ischemia-reperfusion injury (Gasche et al., 2001; Kamada et al., 2007). Several experiments have demonstrated that early inhibition of MMP-9 significantly reduces the brain infarct size, indicating that MMP-9 is an important enzyme in contributing to focal ischemic brain injury (Yong et al., 2001; Tsuji et al., 2005, Klohs et al., 2009; Yagi et al., 2009). We previously reported that the free radical scavenger edaravone shows a protective effect on the NVU reducing MMP-9 activation after tMCAO of rats (Yamashita et al., 2009). Intravenous or intracerebral administration of tPA upregulates MMP-9 and exacerbates cerebral infarction through low-density lipoprotein receptor-related protein (Wang et al., 2003; Kilic et al., 2005; Tsuji et al., 2005; Machado et al., 2009; Yagi et al., 2009; Fanne et al., 2010; Lukic-Panin et al., 2010). The present study demonstrated that administration of tPA at the time of reperfusion

significantly deteriorated the motor function of mice and increased infarct volume especially in the cerebral cortex, and that such clinical and pathological damage by tPA was significantly prevented by administration of nPt (Fig. 1). We further demonstrated that in vivo imaging of MMP activity was well correlated with MMP-9 activity and destruction of NVU after tMCAO, which was also ameliorated by nPt (Fig. 2-4). In the present study, the inner components of NVU such as NAGO and occludin were slightly damaged after tMCAO and administration of tPA as compared to stronger damage in the outer component collagen IV (Fig. 4), similar to our previous report (Yamashita et al., 2009). In the present study the site of ROS production after tMCAO and tPA administration was mainly the cerebrovascular endothelium and neurons, with a few in microglia and astrocytes (Fig. 5a). Both this ROS production and the preferential disruption of NVU were reduced by the present nPt treatment (Fig. 2-5), suggesting that nPt is a potential therapeutic option for ischemic stroke. The present study thus provides evidence for the therapeutic potential of new nPt with both SOD and catalase mimic activities for ischemic stroke patients with NVU protection to improve motor functions through strong antioxidative mechanisms.

Acknowledgements

This work was partly supported by Grant-in-Aid for Scientific Research (B) 21390267 and the Ministry of Education, Science, Culture and Sports of Japan, and by Grants-in-Aid from the Research Committee of CNS Degenerative Diseases (Nakano I), and grants (Itoyama Y, Imai T, Sobue G) from the Ministry of Health, Labour and Welfare of Japan.

References

Abe K (2000), Therapeutic potential of neurotrophic factors and neural stem cells against ischemic brain injury. J Cereb Blood Flow Metab 20: 1393-1408.

Abe K, Kawagoe J, Araki T, Aoki M, Kogure K (1992), Differential expression of heat shock protein 70 gene between the cortex and caudate after transient focal cerebral ischaemia in rats. Neurol Res 14: 381-385.

Abe K, Yuki S, Kogure K (1988), Strong attenuation of ischemic and postischemic brain edema in rats by a novel free radical scavenger. Stroke 19: 480-485.

Abu Fanne R, Nassar T, Yarovoi S, Rayan A, Lamensdorf I, Karakoveski M, Vadim P, Jammal M, Cines DB, Higazi AA (2010), Blood-brain barrier permeability and tPA-mediated neurotoxicity. Neuropharmacology 58: 972-980.

Bederson JB, Pitts LH, Tsuji M, Nishimura MC, Davis RL, Bartkowski H (1986), Rat middle cerebral artery occlusion: evaluation of the model and development of a neurologic examination. Stroke 17: 472–476.

Bindokas VP, Jordán J, Lee CC, Miller RJ (1996), Superoxide production in rat hippocampal neurons: selective imaging with hydroethidine. J Neurosci 16: 1324-1336.

Chan PH (1996), Role of oxidants in ischemic brain damage. Stroke 27: 1124-1129.

Chan PH (2001), Reactive oxygen radicals in signaling and damage in the ischemic brain. J

Cereb Blood Flow Metab 21: 2-14.

Cui J, Holmes EH, Greene TG, Liu PK (2000), Oxidative DNA damage precedes DNA fragmentation after experimental stroke in rat brain. FASEB J 14: 955-967.

Deguchi K, Hayashi T, Nagotani S, Sehara Y, Zhang H, Tsuchiya A, Ohta Y, Tomiyama K, Morimoto N, Miyazaki M, Huh NH, Nakao A, Kamiya T, Abe K. (2008), Reduction of cerebral infarction in rats by biliverdin associated with amelioration of oxidative stress. Brain Res 1188: 1-8.

Demopoulos HB (1973), The basis of free radical pathology. Fed Proc 32: 1859-1861.

Fanne RA, Nassar T, Yarovoi S, Rayan A, Lamensdorf I, Karakoveski M, Vadim P, Jammal M, Cines DB, Higazi AA (2010), Blood-brain barrier permeability and tPA-mediated neurotoxicity. Neuropharmacology 58: 972-980.

Gasche Y, Copin JC, Sugawara T, Fujimura M, Chan PH (2001), Matrix metalloproteinase inhibition prevents oxidative stress-associated blood-brain barrier disruption after transient focal cerebral ischemia. J Cereb Blood Flow Metab 21: 1393-1400.

Hamasaki T, Kashiwagi T, Imada T, Nakamichi N, Aramaki S, Toh K, Morisawa S, Shimakoshi H, Hisaeda Y, Shirahata S (2008), Kinetic analysis of superoxide anion radical-scavenging and hydroxyl radical-scavenging activities of platinum nanoparticles. Langmuir 24: 7354-7364.

Hayashi T, Hamakawa K, Nagotani S, Jin G, Li F, Deguchi K, Sehara Y, Zhang H, Nagano I, Shoji M, Abe K (2005), HMG CoA reductase inhibitors reduce ischemic brain injury of Wistar

rats through decreasing oxidative stress on neurons. Brain Res 1037: 52-58.

Hayashi T, Sakurai M, Itoyama Y, Abe K (1999), Oxidative damage and breakage of DNA in rat brain after transient MCA occlusion. Brain Res 832: 159-163.

Hsiao G, Lee JJ, Chen YC, Lin JH, Shen MY, Lin KH, Chou DS, Sheu JR (2007), Neuroprotective effects of PMC, a potent alpha-tocopherol derivative, in brain ischemia-reperfusion: reduced neutrophil activation and anti-oxidant actions. Biochem Pharmacol 73: 682-693.

Kajita M, Hikosaka K, Iitsuka M, Kanayama A, Toshima N, Miyamoto Y (2007), Platinum nanoparticle is a useful scavenger of superoxide anion and hydrogen peroxide. Free Radic Res 41: 615-626.

Kamada H, Yu F, Nito C, Chan PH (2007), Influence of hyperglycemia on oxidative stress and matrix metalloproteinase-9 activation after focal cerebral ischemia/reperfusion in rats. Stroke 38: 1044-1049.

Kilic E, Kilic Ü, Bähr M, Hermann DM (2005), Tissue plasminogen activator-induced ischemic injuly is reversed by NMDA antagonist MK-801 in vivo. Neurodegenerative Dis 2: 49-55.

Kilic E, Kilic U, Matter CM, Lüscher TF, Bassetti CL, Hermann DM (2005), Aggravation of focal cerebral ischemia by tissue plasminogen activator is reversed by 3-hydroxy-3-methylglutaryl coenzyme A reductase inhibitor but does not depend on endothelial NO synthase. Stroke 36: 332-336.

Kim J, Shirasawa T, Miyamoto Y (2010), The effect of TAT conjugated platinum nanoparticles on lifespan in a nematode Caenorhabditis elegans model. Biomaterials 31: 5849-5854.

Kim J, Takahashi M, Shimizu T, Shirasawa T, Kajita M, Kanayama A, Miyamoto Y (2008), Effects of a potent antioxidant, platinum nanoparticle, on the lifespan of Caenorhabditis elegans. Mech Ageing Dev 129: 322-331.

Kinouchi H, Epstein CJ, Mizui T, Carlson E, Chen SF, Chan PH (1991), Attenuation of focal cerebral ischemic injury in transgenic mice overexpressing CuZn superoxide dismutase. Proc Natl Acad Sci U S A 88: 11158–11162.

Klohs J, Steinbrink J, Bourayou R, Mueller S, Cordell R, Licha K, Schirner M, Dirnagl U, Lindauer U, Wunder A (2009), Near-infrared fluorescence imaging with fluorescently labeled albumin: a novel method for non-invasive optical imaging of blood-brain barrier impairment after focal cerebral ischemia in mice. J Neurosci Methods 180: 126-132.

Kontos CD, Wei EP, Williams JI, Kontos HA, Povlishock JT (1992), Cytochemical detection of superoxide in cerebral inflammation and ischemia in vivo. Am J Physiol 263: 1234–1242.

Kontos HA (2001), Oxygen radicals in cerebral ischemia. Stroke 32: 2712–2716.

Lansberg MG, Bluhmki E, Thijs VN (2009), Efficacy and safety of tissue plasminogen activator 3 to 4.5 hours after acute ischemic stroke: a metaanalysis. Stroke 40: 2438-2441.

Lukic-Panin V, Deguchi K, Yamashita T, Shang J, Zhang X, Tian F, Liu N, Kawai H, Matsuura T, Abe K (2010), Free radical scavenger edaravone administration protects against tissue plasminogen activator induced oxidative stress and blood brain barrier damage. Curr Neurovasc Res 7: 319-329.

Lukic-Panin V, Kamiya T, Zhang H, Hayashi T, Tsuchiya A, Sehara Y, Deguchi K, Yamashita T, Abe K (2007), Prevention of neuronal damage by calcium channel blockers with antioxidative effects after transient focal ischemia in rats. Brain Res 1176: 143-150.

Machado LS, Sazonova IY, Kozak A, Wiley DC, El-Remessy AB, Ergul A, Hess DC, Waller JL, Fagan SC (2009), Minocycline and tissue-type plasminogen activator for stroke: assessment of interaction potential. Stroke 40: 3028-3033.

Morimoto T, Globus MY, Busto R, Martinez E, Ginsberg MD (1996), Simultaneous measurement of salicylate hydroxylation and glutamate release in the penumbral cortex following transient middle cerebral artery occlusion in rats. J Cereb Blood Flow Metab 16: 92-99.

Nagai N, De Mol M, Lijnen HR, Carmeliet P, Collen D (1999), Role of plasminogen system components in focal cerebral ischemic infarction: a gene targeting and gene transfer study in mice. Circulation 99: 2440-2444.

Nagotani S, Hayashi T, Sato K, Zhang W, Deguchi K, Nagano I, Shoji M, Abe K (2005), Reduction of cerebral infarction in stroke-prone spontaneously hypertensive rats by statins

associated with amelioration of oxidative stress. Stroke 36: 670-672.

Ning M, Furie KL, Koroshetz WJ, Lee H, Barron M, Lederer M, Wang X, Zhu M, Sorensen AG, Lo EH, Kelly PJ (2006), Association between tPA therapy and raised early matrix metalloproteinase-9 in acute stroke. Neurology 66: 1550-1555.

Onizawa S, Aoshiba K, Kajita M, Miyamoto Y, Nagai A (2009), Platinum nanoparticle antioxidants inhibit pulmonary inflammation in mice exposed to cigarette smoke. Pulm Pharmacol Ther 22: 340-349.

Perfeito R, Pereira J, Oliveira CR, Bettencourt-Relvas J, Rego AC (2007), Trolox protection of myelin membrane in hydrogen peroxide-treated mature oligodendrocytes. Free Radic Res 41: 444-451.

Peters O, Back T, Lindauer U, Busch C, Megow D, Dreier J, Dirnagl U (1998), Increased formation of reactive oxygen species after permanent and reversible middle cerebral artery occlusion in the rat. J Cereb Blood Flow Metab 18: 196–205.

Roucoux A, Schulz J, Patin H (2002), Reduced transition metal colloids: a novel family of reusable catalysts? Chem Rev 102: 3757-3778.

Saitoh Y, Yoshimura Y, Nakano K, Miwa N (2009), Platinum nanocolloid-supplemented hydrogen- dissolved water inhibits growth of human tongue carcinoma cells preferentially over normal cells. Exp Oncol 31: 156-162.

Sakaue Y, Kim J, Miyamoto Y (2010), Effects of TAT-conjugated platinum nanoparticles on lifespan of mitochondrial electron transport complex I-deficient Caenorhabditis elegans, nuo-1. Int J Nanomedicine 5: 687-695.

Sharma SS, Kaundal RK (2007), Neuroprotective effects of 6-hydroxy-2,5,7,8-tetramethyl-chroman-2-carboxylic acid (Trolox), an antioxidant in middle cerebral artery occlusion induced focal cerebral ischemia in rats. Neurol Res 29: 304-309.

Sugawara T, Noshita N, Lewén A, Gasche Y, Ferrand-Drake M, Fujimura M, Morita-Fujimura Y, Chan PH (2002), Overexpression of copper/zinc superoxide dismutase in transgenic rats protects vulnerable neurons against ischemic damage by blocking the mitochondrial pathway of caspase activation. J Neurosci 22: 209-217.

Takamiya M, Miyamoto Y, Yamashita T, Deguchi K, Ohta Y, Ikeda Y, Matsuura T, Abe K (2011), Neurological and pathological improvements of cerebral infarction in mice with platinum nanoparticles. J Neurosci Res 89: 1125-1133.

The Edaravone Acute Brain Infarction Study Group (2003), Effect of a novel free radical scavenger, edaravone (MCI-186), on acute brain infarction. Randomized, placebo-controlled, double-blind study at multicenters. Cerebrovasc Dis 15: 222–229.

Tsirka SE, Gualandris A, Amaral DG, Strickland S (1995), Excitotoxin-induced neuronal degeneration and seizure are mediated by tissue plasminogen activator. Nature 377: 340-344.

Tsuji K, Aoki T, Tejima E, Arai K, Lee SR, Atochin DN, Huang PL, Wang X, Montaner J, Lo EH (2005), Tissue plasminogen activator promotes matrix metalloproteinase-9 upregulation after focal cerebral ischemia. Stroke 36: 1954-1959.

Wahlgren N, Ahmed N, Davalos A, Hacke W, Milian M, Muir K, Roine RO, Toni D, Lees KR; SITS investigators (2008), SITS investigators. Thrombolysis with alteplase 3-4.5 h after acute ischaemic stroke (SITS-ISTR): an observational study. Lancet 372: 1303-1309.

Wang X, Lee SR, Arai K, Tsuji K, Rebeck GW, Lo EH (2003), Lipoprotein receptor-mediated induction of matrix metalloproteinase by tissue plasminogen activator. Nat Med 9: 1313-1317.

Wang YF, Tsirka SE, Strickland S, Stieg PE, Soriano SG, Lipton SA (1998), Tissue plasminogen activator (tPA) increases neuronal damage after focal cerebral ischemia in wild-type and tPA-deficient mice. Nat Med 4: 228-231.

Watanabe A, Kajita M, Kim J, Kanayama A, Takahashi K, Mashino T, Miyamoto Y (2009), In vitro free radical scavenging activity of platinum nanoparticles. Nanotechnology 20: 455105.

Yagi K, Kitazato KT, Uno M, Tada Y, Kinouchi T, Shimada K, Nagahiro S (2009), Edaravone, a free radical scavenger, inhibits MMP-9-related brain hemorrhage in rats treated with tissue plasminogen activator. Stroke 40: 626-631.

Yamashita T, Deguchi K, Sawamoto K, Okano H, Kamiya T, Abe K (2006), Neuroprotection and neurosupplementation in ischaemic brain. Biochem Soc Trans 34: 1310-1312.

Yamashita T, Kamiya T, Deguchi K, Inaba T, Zhang H, Shang J, Miyazaki K, Ohtsuka A, Katayama Y, Abe K (2009), Dissociation and protection of the neurovascular unit after thrombolysis and reperfusion in ischemic rat brain. J Cereb Blood Flow Metab 29: 715-725.

Yoneda Y, Uehara T, Yamasaki H, Kita Y, Tabuchi M, Mori E (2003), Hospital-based study of the care and cost of acute ischemic stroke in Japan. Stroke 34: 718-724.

Yong VW, Power C, Forsyth P, Edwards DR **(**2001), Metalloproteinases in biology and pathology of the nervous system. Nat Rev Neurosci 2: 502-511.

Zhang WR, Hayashi T, Sasaki C, Sato K, Nagano I, Manabe Y, Abe K (2001), Attenuation of oxidative DNA damage with a novel antioxidant EPC-K1 in rat brain neuronal cells after transient middle cerebral artery occlusion. Neurol Res 23: 676-680.

Zhang WR, Sato K, Hayashi T, Omori N, Nagano I, Kato S, Horiuchi S, Abe K (2004), Extension of ischemic therapeutic time window by a free radical scavenger,edaravone, reperfused with tPA in rat brain. Neurol Res 26: 342–348.

Figure legends

Figure 1. Neurobehavioral analysis and infarct volume

Quantitative analysis of (A) Bederson's motor grade, (B) rota rod motor score, and (C) infarct volume at 48 hrs after tMCAO. Compared with the sham control group, the motor function of the tMCAO-vehicle group showed a strong reduction of motor scores (⋆⋆$p < 0.01$), with further exacerbation in the tMCAO-tPA group (*$p < 0.05$, **$p < 0.01$). Treatment with nPt showed a significant improvement (#$p < 0.05$, ##$p < 0.01$ tMCAO-tPA vs tMCAO-tPA+nPt group; *$p < 0.05$, **$p < 0.01$ vs tMCAO-vehicle group) (A and B). The infarct volume in the cerebral cortex and caudoputamen (CPu) showed inverse results (*$p < 0.05$, **$p < 0.01$ vs tMCAO-vehicle group; #$p < 0.05$, ##$p < 0.01$ tMCAO-tPA vs tMCAO-tPA+nPt group) (C).

Figure 2. MMP-9 in vivo and ex vivo optical imaging

In vivo optical images of MMP at 48 hrs after tMCAO (A) with skull bone, (B) ex vivo optical imaging of whole brain, and (C) the coronal brain slice (upper panels for non-fluorescence pictures, and lower panels for pseudocolor images). Note the strong fluorescent signal in the right hemisphere reflecting the affected right MCA territory of tMCAO groups, the strongest in tMCAO-tPA group, and the great reduction by nPt treatment (A-C, lower panels). Macroscopic comparison of brain sections with TTC stain and ex vivo MMP image in identical tMCAO-tPA mice showed close colocalization of TTC stain defect (D, upper panel, white area)

and MMP image increase (D, lower panel, yellow area). Microscopic fluorescent observation confirmed the colocalization of endogenous MMPSense signals and exogenous MMP-9 antibody in the affected area (E). Bar indicates 50 μm.

Figure 3. Gelatine zymography

Representative zymogram for MMP-9 at 48 hrs after tMCAO (A), and its densitometric analysis (B). Note the remarkable activation of MMP-9 in the ipsilateral hemisphere of the tMCAO-vehicle group compared with the sham control group ($\star p < 0.05$), a significant aggravation in the tMCAO-tPA group ($*p < 0.05$), and a great reduction in nPt groups ($*p < 0.05$ vs tMCAO-vehicle group, $\#p < 0.05$ tMCAO-tPA vs tMCAO-tPA+nPt group).

Figure 4. Immunohistochemistry

Representative photomicrographs for NAGO, occludin, collagen IV and MMP-9 immunostaining of the peri-infarct areas of mouse brains in sham control, tMCAO-vehicle, tMCAO-tPA, tMCAO-tPA+nPt, and tMCAO-nPt groups. Bar indicates 50 μm. Quantitative analysis of the signal intensity compared to sham control are shown in the right, showing a significant decrease (collagen IV) and an increase (MMP-9) in the tMCAO-vehicle group, an aggravation in the tMCAO-tPA group, and an improvement by the nPt treatment ($\star p < 0.05$, $\star\star p < 0.01$ vs sham control; $*p < 0.05$, $**p < 0.01$ vs tMCAO-vehicle group; $\#p < 0.05$, $\#\#p < 0.01$ tMCAO-tPA vs tMCAO-tPA+nPt group).

Figure 5. Hydroethidine stain

Quantitative analysis of the ethidium signals in endothelium, neuron, astrocyte, and microglia of hydroethidine-stained coronal brain sections at 2 hrs after tMCAO (A) and representative fluorescent photomicrographs for hydroethidine, MAP2, CD31, and merged image of the peri-infarct areas of mouse brains. Bar indicates 10 μm (B). Note strong signals by hydroethidine in the endothelium of tMCAO-vehicle and tMCAO-tPA groups (filled arrows), and a much lower intensity by nPt treatment (open arrows) (B). ⋆$p < 0.05$, ⋆⋆$p < 0.01$ vs sham control; *$p < 0.05$, **$p < 0.01$ vs tMCAO-vehicle group; #$p < 0.05$ tMCAO-tPA vs tMCAO-tPA+nPt group.

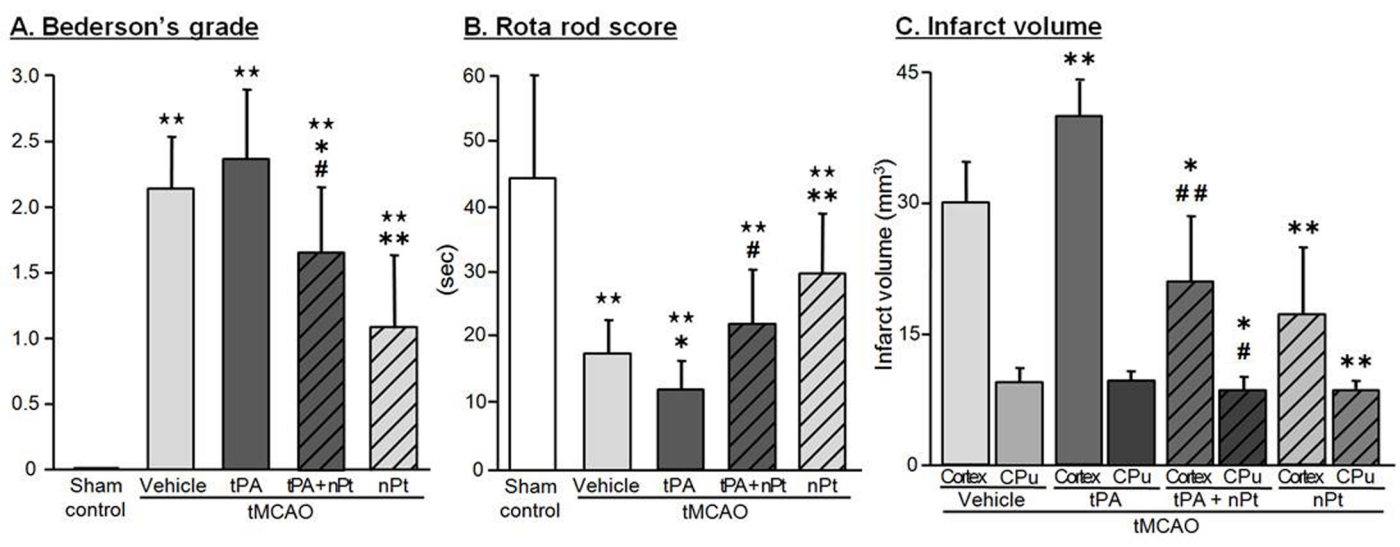
A. Bederson's grade
3.0
2.5
2.0
1.5
1.0
0.5
0
Sham control
Vehicle
tPA
tPA+nPt
nPt
tMCAO
B. Rota rod score
(sec)
60
50
40
30
20
10
0
Sham control
Vehicle
tPA
tPA+nPt
nPt
tMCAO
C. Infarct volume
Infarct volume (mm3)
45
30
15
0
Cortex
CPu
Vehicle
tPA
tPA + nPt
nPt
tMCAO

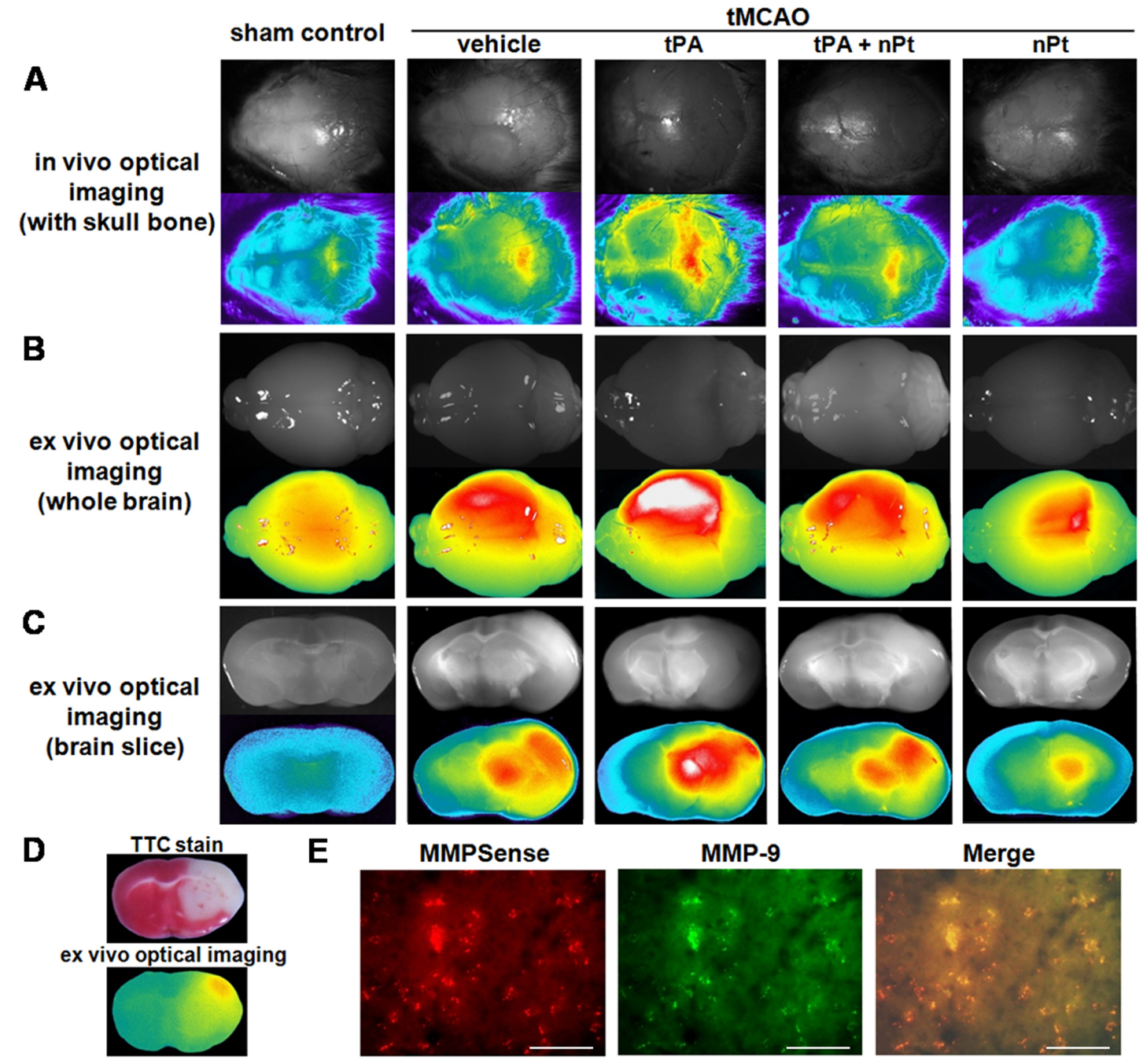
sham control
tMCAO
vehicle
tPA
tPA + nPt
nPt
A
in vivo optical imaging (with skull bone)
B
ex vivo optical imaging (whole brain)
C
ex vivo optical imaging (brain slice)
D
TTC stain
ex vivo optical imaging
E
MMPSense
MMP-9
Merge

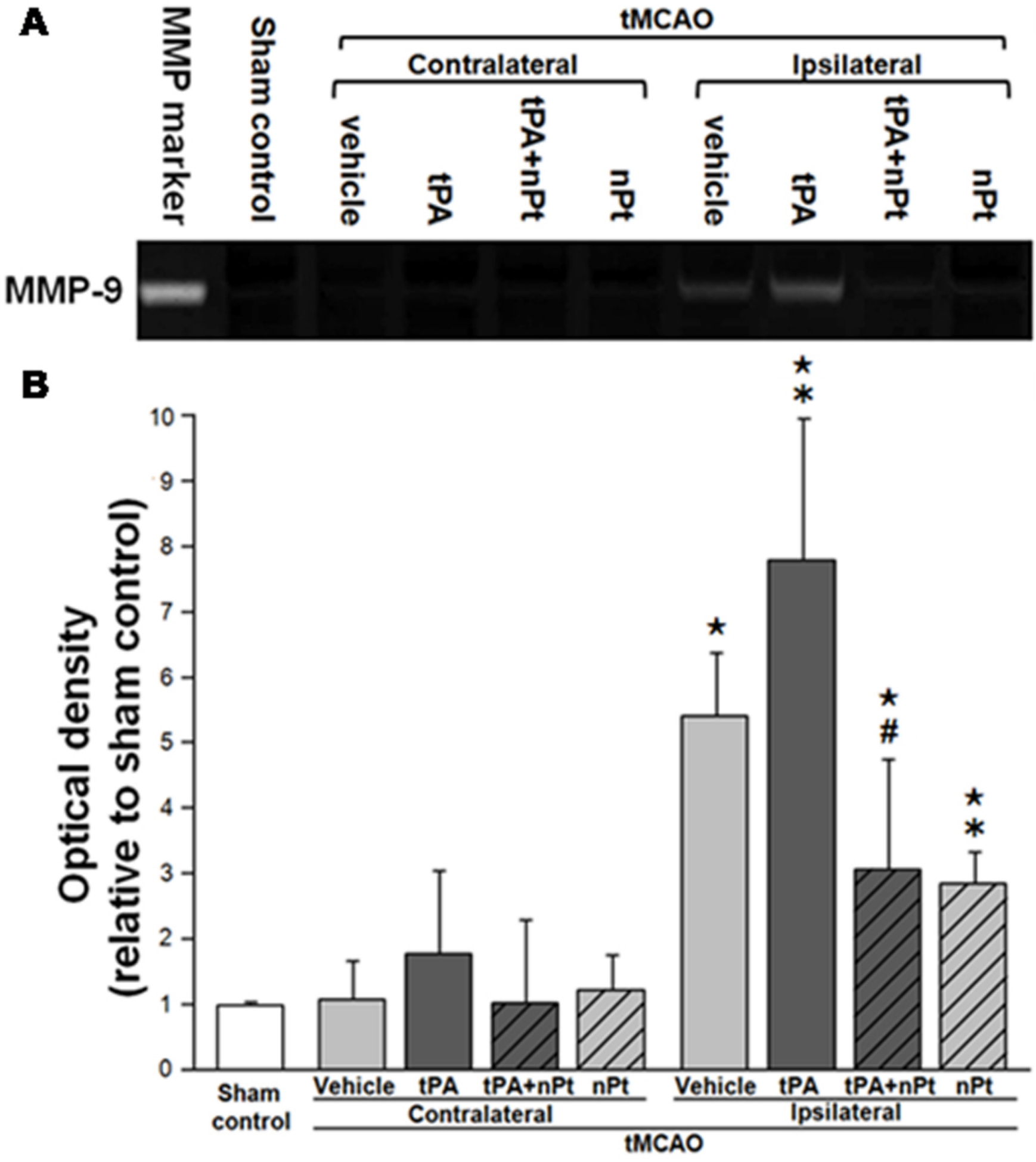
A
MMP marker
Sham control
tMCAO
Contralateral
Ipsilateral
vehicle
tPA
tPA+nPt
nPt
vehicle
tPA
tPA+nPt
nPt
MMP-9
B
Optical density
(relative to sham control)
0
1
2
3
4
5
6
7
8
9
10
Sham control
Vehicle
tPA
tPA+nPt
nPt
Vehicle
tPA
tPA+nPt
nPt
Contralateral
Ipsilateral
tMCAO

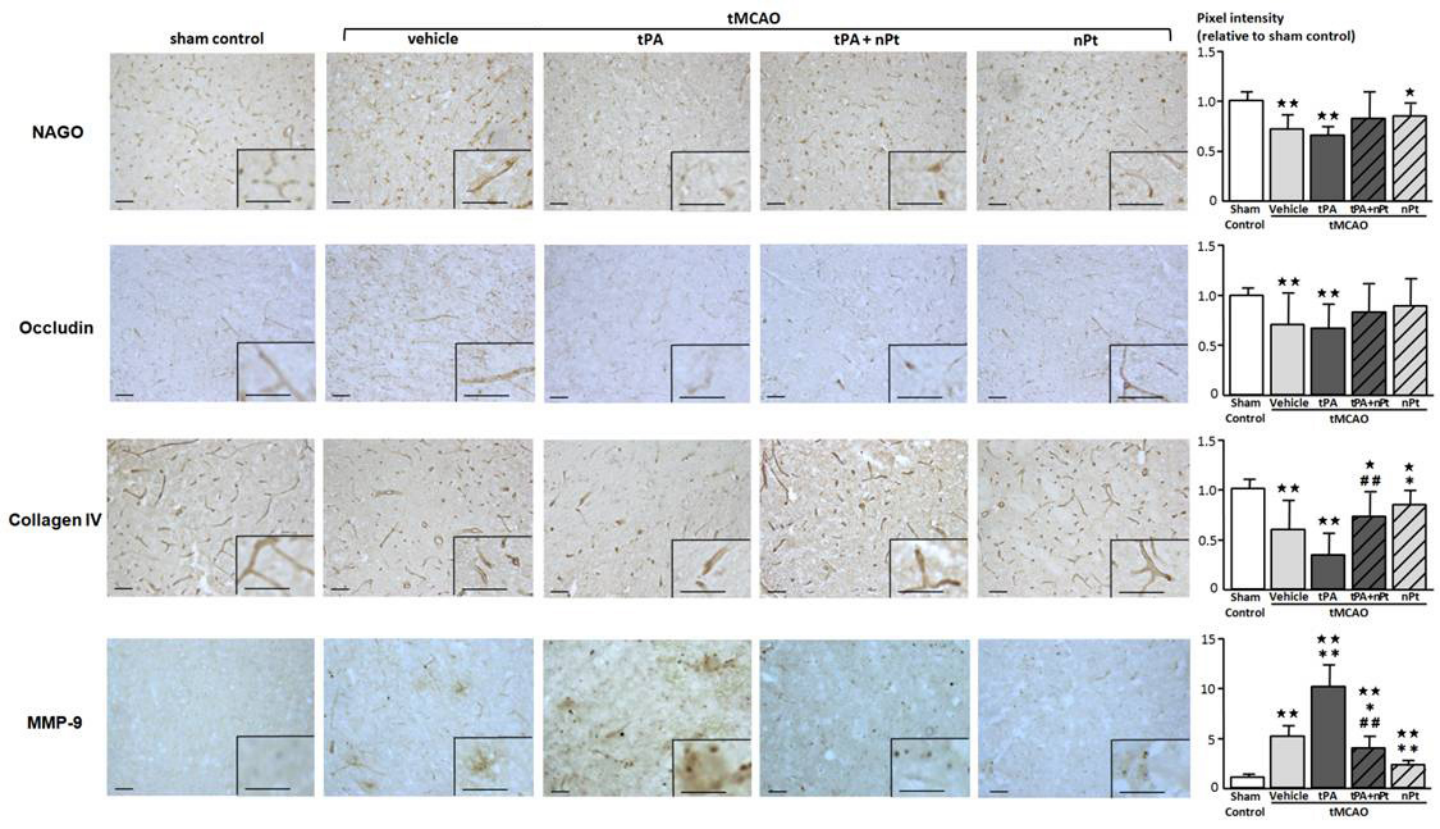
sham control
tMCAO
vehicle
tPA
tPA + nPt
nPt
Pixel intensity
(relative to sham control)
NAGO
Occludin
Collagen IV
MMP-9
Sham Control
Vehicle
tPA
tPA+nPt
nPt
tMCAO

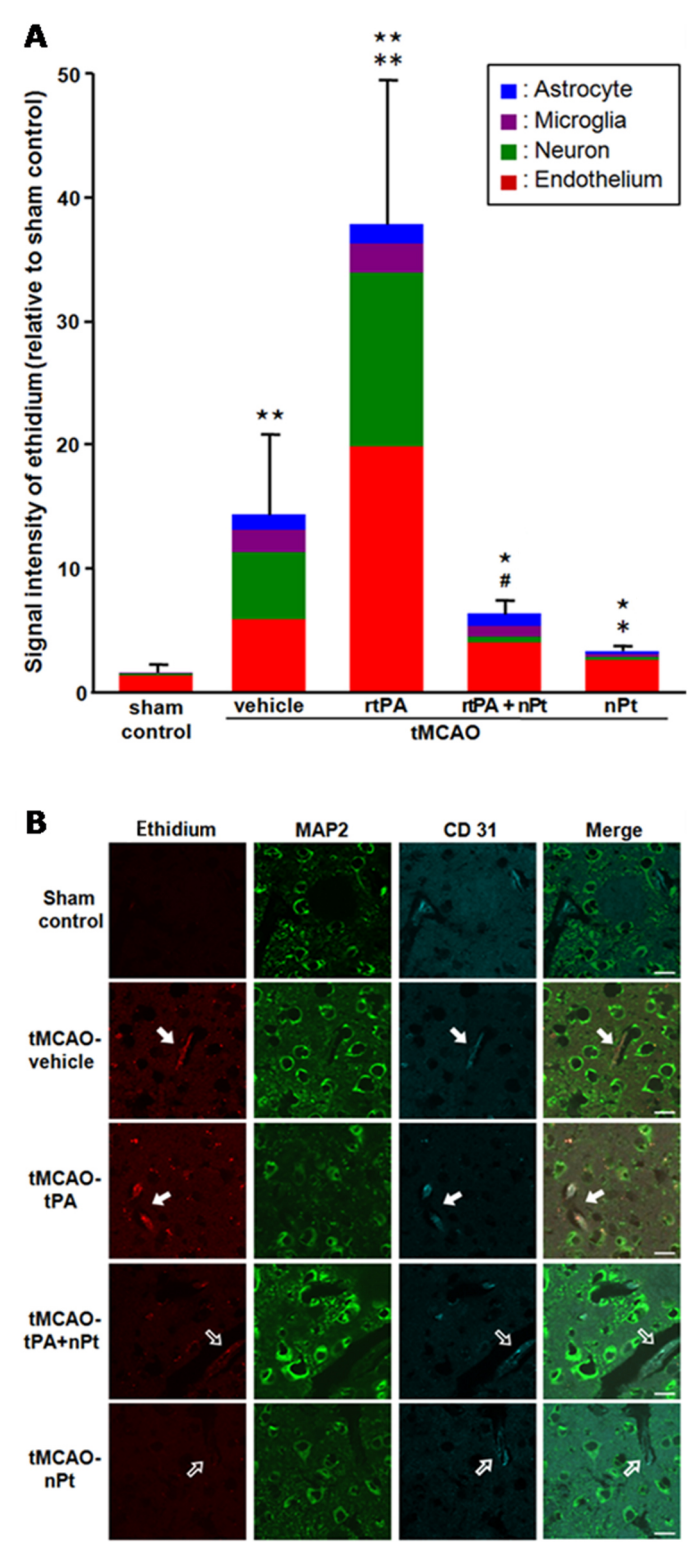
A
Signal intensity of ethidium (relative to sham control)
50
40
30
20
10
0
: Astrocyte
: Microglia
: Neuron
: Endothelium
**
**
**
*
#
*
*
sham control
vehicle
rtPA
rtPA + nPt
nPt
tMCAO
B
Ethidium
MAP2
CD 31
Merge
Sham control
tMCAO-vehicle
tMCAO-tPA
tMCAO-tPA+nPt
tMCAO-nPt